NUCLEAR SCIENCE AND ENGINEERING: **173**, 43–57 (2013)

# Determination and Application of Partial Biases in Criticality Safety Validation

Jeremy A. Roberts*

*University of Wisconsin–Madison, Department of Engineering Physics*
*1500 Engineering Drive, Madison, Wisconsin 53706*

Bradley T. Rearden

*Oak Ridge National Laboratory*
*Oak Ridge, Tennessee 37831-6470*

and

Paul P. H. Wilson

*University of Wisconsin–Madison, Department of Engineering Physics*
*1500 Engineering Drive, Madison, Wisconsin 53706*

*Received December 16, 2010*
*Accepted April 21, 2012*

**Abstract**—*This paper presents a method for determining partial biases and bias uncertainties for application in fission product burnup credit criticality safety analysis. The contribution of each nuclide to the overall system $k_{eff}$ bias and the bias uncertainty are determined via the generalized linear least squares method. Where experimental benchmarks are available to validate specific nuclides, sensitivity and uncertainty analysis is used to project biases observed in the benchmarks to biases appropriate for the safety system. Two weighting schemes are proposed to produce an overall bias in the safety system from several single partial biases. Finally, these methods are used to determine partial biases for $^{149}$Sm and $^{103}$Rh from two experiment series and to apply these biases to a representative used fuel safety system. The biases obtained are compared to bounding estimates, and the sensitivity of the results to relevant assumptions is addressed.*

## I. INTRODUCTION

To predict or bound the computational bias for a safety system of interest, one may utilize American National Standards ANSI/ANS-8.1-1998 (Ref. 1), and ANSI/ANS-8.24-2007 (Ref. 2), which allow the use of calculations in the determination of subcritical limits for the design of fissionable material systems. A computational bias is the difference between the computed and the actual values of a parameter, invariably $k_{eff}$. The aforementioned standards require validation of the analytical methods and data used in nuclear criticality safety calculations to quantify any computational bias and the uncertainty in the bias. The validation procedure must be conducted through comparison of the computed results with experimental data, and the safety system must be sufficiently similar to the experiments to be within the area of applicability of the experiments chosen for validation. ANSI/ANS-8.1-1998 defines the area (or areas) of applicability as "the limiting ranges of material compositions, geometric arrangements, neutron-energy spectra, and other relevant parameters (e.g., heterogeneity, leakage, interaction, absorption, etc.) within which the bias of a computational method is established."

Traditionally, the similarity of systems is determined via comparison of several parameters deemed

*E-mail: robertsj@mit.edu

adequate estimators of the likeness between two systems. For example, energy of average lethargy causing fission and hydrogen-to-fissile atom ratios have long been used in criticality safety analyses; more recently, parameters based on sensitivity and uncertainty (S/U) analysis have been used, including $c_k$, $E$, and others.[3] A computational bias can be found as a function of such trending parameters, and a statistical analysis can be used to determine an upper subcritical limit.

Unfortunately, a different approach to bias determination is needed to include credit for fission products (FPs) in safety analyses for full burnup credit, that is, accounting for the reduction in $k_{eff}$ due to both actinide changes and FPs in criticality safety analyses. The importance of full burnup credit for transportation and storage of used nuclear fuel has been well-established elsewhere.[4]

Ideally, critical experiments for full burnup credit would involve U, Pu, and FPs in isotopic ratios similar to those found in used nuclear fuel. However, such experiments are not available and will not likely be conducted. Further, many FPs present in used nuclear fuel have only a small effect on the $k_{eff}$ value of the system. FPs need to be present in larger quantities in critical experiments so that a FP bias due to nuclear data errors is statistically significant in critical experiment models. Consequently, a method is needed to isolate the contribution of an individual FP to the total computational bias (i.e., partial bias) of an experiment model and to apply such a bias to safety analysis systems. In other words, it is necessary to compute partial FP biases using single FP experiments that are already available for some nuclides and more likely to be conducted for additional nuclides and to apply such biases, in some manner, to application systems of interest.

This paper develops methods both to determine partial biases from experiments and to apply those biases to application systems. In doing so, a fundamental assumption made is that the computational bias is due solely (or at least mostly) to errors in the cross-section data. Previous analysis demonstrated that cross-section uncertainties, when propagated to $k_{eff}$ via sensitivities, establish bounding estimates for computational biases, which suggests that biases are in fact due to cross-section uncertainty.[5] Where other nonnegligible systematic biases exist, such as those from modeling or other approximations, a method to quantify or otherwise eliminate these contributions to the total bias is needed.

The organization of this paper is as follows. First, an overview of relevant S/U tools and quantities is given, and a new integral index is defined to quantify similarity between a safety system and an experiment with respect to their $k_{eff}$ sensitivities to a single nuclide reaction. Thereafter, an approach for extracting partial biases from experimental data is described that uses the generalized linear least squares (GLLS) technique. These (individual) partial biases are simultaneously propagated to the safety system of interest using sensitivity data. Two weighting schemes are then presented for producing a single effective application bias from several individual biases. The methods are subsequently demonstrated using two available FP experiments and a representative used fuel model, followed by a discussion of the sensitivity of the results to various assumptions.

## II. SENSITIVITY ANALYSIS

The SCALE code system,[6] developed by Oak Ridge National Laboratory (ORNL), contains modules for performing eigenvalue sensitivity analysis, known as Tools for Sensitivity and Uncertainty Analysis Methodology Implementation (TSUNAMI). The TSUNAMI-3D sequence uses Monte Carlo neutron transport to compute eigenvalue sensitivities to perturbations in nuclear data for arbitrary three-dimensional geometry. This section defines sensitivity coefficients for both $k_{eff}$ and eigenvalue differences. Additionally, use of sensitivity coefficients in nuclide-specific integral parameters is discussed.

### *II.A. Sensitivity Coefficients*

As implemented in TSUNAMI, the $k_{eff}$ sensitivity to perturbations in infinitely dilute cross-section data $\sigma_j$ is defined by

$$S_j = \frac{\Delta k/k}{\Delta\sigma_j/\sigma_j} \tag{1}$$

for an energy group $j$. Here, $S_j$ is defined for a single nuclide reaction, e.g., elastic scattering for $^1$H. Thus, $S_j$ is an energy-dependent function, referred to subsequently as a sensitivity profile. Integrating $S_j$ over energy yields the total or integrated sensitivity coefficient.

### *II.B. Eigenvalue-Difference Response Sensitivities*

Another SCALE module, the Tool for Sensitivity Analysis of Reactivity (TSAR), generates sensitivity coefficients for eigenvalue-difference responses, e.g., reactivity, and the basic theory has been well documented elsewhere.[7] The reactivity of a given reactor state 1 is defined by

$$\rho_1 = 1 - \frac{1}{k_1} = 1 - \lambda_1 \tag{2}$$

and is defined similarly for a second state. For the purposes of this paper, the first state is an experiment with no FP present (NFP), and a second state would be a nearly identical system with a FP present.

The "reactivity" between states 1 and 2 is defined as the reactivity difference

$$\rho_{1\to 2} = \rho_1 - \rho_2 = \lambda_2 - \lambda_1 \ , \tag{3}$$

and the associated sensitivity of $\rho_{1\to 2}$ to perturbations in a given nuclide-reaction cross section is defined as

$$S_{\rho_{1\to 2}} = \frac{\lambda_1 S_{\lambda_1} - \lambda_2 S_{\lambda_2}}{\rho_{1\to 2}} = \frac{k_1 S_{k_2} - k_2 S_{k_1}}{\rho_{1\to 2}} \ . \tag{4}$$

These reactivity sensitivities are computed using the standard $k_{eff}$ sensitivities generated by TSUNAMI and will be of importance below.

### *II.C. Nuclide-Reaction Integral Indices*

To compare the qualitative similarity between applications (e.g., a used fuel canister) and (critical) experiment $k_{eff}$ sensitivities to a particular nuclide, we define a new integral index not implemented in SCALE as

$$\hat{g} = 1 - \frac{\sum_j^G |S_j^a - \tilde{S}_j^e|}{\sum_j^G |S_j^a|} \ , \tag{5}$$

where

$a, e$ = application and experiment, respectively

$G$ = total number of energy groups

and the experiment sensitivity has been normalized such that

$$\tilde{S}_j^e = S_j^e \times \frac{\sum_j^G S_j^a}{\sum_j^G S_j^e} \ . \tag{6}$$

Experiments having a high $\hat{g}$ for a given application exhibit sensitivities in $k_{eff}$ that are highly consistent with the $k_{eff}$ sensitivities of the application for the given nuclide reaction. Such consistency is important because it means that the bias due to data errors for the nuclide reaction in the experiment has the same energy dependence as the application system bias for the nuclide reaction. A value $\hat{g} = 1$ indicates complete similarity, $\hat{g} = 0$ indicates complete dissimilarity, and $\hat{g} = -1$ indicates complete "antisimilarity."

The interpretation of $\hat{g}$ can be compared to the integral index $g$, which measures the "coverage" that an experiment provides for a certain nuclide reaction as implemented in the SCALE TSUNAMI Indices and Parameters (TSUNAMI-IP) code. The index $g$ is defined as[8]

$$g = 1 - \frac{\sum_j^G \tilde{Z}_j}{\sum_j^G S_j^a} \ , \tag{7}$$

where

$$\tilde{Z}_j = \begin{cases} S_j^a - S_j^e & \text{if } |S_j^a| > |S_j^e|, \\ 0 & \text{otherwise} \ . \end{cases} \tag{8}$$

Coverage is defined as those energy groups over which $S_j^e > S_j^a$, and hence, $g$ quantifies the coverage provided for a nuclide reaction. Undercoverage or noncoverage can be penalized with a penalty defined as

$$p_g = \sqrt{\tilde{\mathbf{Z}} \mathbf{C}_{\alpha\alpha} \tilde{\mathbf{Z}}^T} \ , \tag{9}$$

where

$\tilde{\mathbf{Z}}$ = vector of all groupwise sensitivity differences $\tilde{Z}_j$ for all nuclides

$\mathbf{C}_{\alpha\alpha}$ = cross-section covariance matrix, consisting of relative variances (main diagonal entries) and covariances (off-diagonal entries) of the cross-section data.

This penalty can be added to the computational bias in safety analyses but is only applicable for undercoverage. In the case where $S_j^a < S_j^e$, overcoverage exists, which is not accounted for in this penalty calculation.

Unlike $\hat{g}$, $g$ takes into account only the difference between the experiment and application sensitivities and consequently does not account for the energy dependence and hence consistency between the change in $k_{eff}$ due to errors in the nuclide-reaction data. Accounting for this consistency is important when analyzing single nuclide reactions independent of other system features. For example, a given experiment might have a particular nuclide present at significantly higher concentrations than an application, and so, the integrated sensitivity coefficient and hence overall sensitivity profile will be much larger than the application profile regardless of the similarity in shape. If the shapes of the profiles are not similar, then the effect on $k_{eff}$ due to errors in the nuclide-reaction data will not be the same, and so, the partial bias found for an experiment is not applicable to the application system. In this paper, we deal with biases as a function of energy and therefore never compare (total) partial biases explicitly; even so, it remains highly desirable to have consistent biases or, equivalently, experiments with a high $\hat{g}$ for a safety system.

Analogous to $p_j$, a penalty for nonsimilarity as quantified by $\hat{g}$ can be written

$$p_{\hat{g}} = \sqrt{\hat{\mathbf{Z}} \mathbf{C}_{\alpha\alpha} \hat{\mathbf{Z}}^T} \ , \tag{10}$$

where $\hat{\mathbf{Z}} = \mathbf{S}^{\mathbf{a}} - \tilde{\mathbf{S}}^{\mathbf{e}}$. Hence, $p_{\hat{g}}$ penalizes the area over which the application and normalized experiment sensitivity profiles do not overlap. It turns out that $p_{\hat{g}}$ is not a completely accurate expression for a penalty due to nonsimilarity; the proper expression is derived below in the context of partial bias application. We include it here for comparison only.

## III. BIAS ASSESSMENT WITH GLLS TECHNIQUES

A new capability for SCALE 6 allows the prediction of computational biases with the nuclear data adjustment tool TSURFER, which is based on a GLLS approach.[9] The data adjustments in TSURFER are not used to produce adjusted cross-section data libraries for subsequent use; rather, they are used only to predict biases in application systems. As TSURFER is a general-purpose tool, a computed quantity for which a bias is predicted is referred to as a response. A response is often $k_{eff}$ but in general could be reactivity, a reaction rate ratio, or any other quantity of interest that can be both measured in benchmark experiments and calculated through numerical simulation using multigroup cross-section data.

TSURFER operates on data from a series of benchmark experiments included as experiment responses. The measured responses, their uncertainties, and correlations are input to TSURFER as well as the calculated values, their uncertainties, and sensitivities. Cross-section covariance data are also included. TSURFER identifies a single set of adjustments to nuclear data and experimental values, all bounded by their uncertainties, that will result in the computational models all producing response values close to their experimental response value, in essence eliminating the biases in the experiments. Then, the same data adjustments that result in unbiased calculations for the experiments are used to predict an unbiased response value for the application and an uncertainty on the adjusted response value. The difference between the originally calculated response value and the new postadjustment response value represents the bias in the original calculation, and the uncertainty in the adjusted value represents the uncertainty in this bias.

A typical use of the GLLS method (GLLSM) has been to determine the bias of an application $k_{eff}$. Such analysis requires a single set of benchmark experiments similar to the application system and for which measured and computed responses are available. The resulting data adjustments are then used to compute the application bias. Note that the required data and their subsequent use differ somewhat for determination of partial biases, as explained in Sec. III.C.

If similar experiments are available to validate the use of a particular nuclide in the application, the uncertainty of the bias for this nuclide is reduced. In TSURFER, experiments that are dissimilar from the application can still provide useful information for bias assessment if at least one material demonstrates similar sensitivities to those of the application. If similar experiments are not available to validate a particular nuclide, a high uncertainty in the bias for the given nuclide will result. Thus, with a complete set of experiments to validate important components in the application, a precise bias with a small uncertainty can be predicted. Where the experimental coverage is lacking, a bias can be predicted with an appropriately large uncertainty.

As users gain experience with TSURFER, it may become a preferred tool for rigorous bias and bias uncertainty determination, particularly for applications for which nearly identical critical experiments are not available. However, the results of TSURFER analyses rely on the availability of quality uncertainty and correlation data for both nuclear data and benchmark experiments. The GLLS techniques implemented in TSURFER are documented elsewhere and will not be repeated here.[10]

### *III.A. Expressions for Computational Bias*

The computational bias for experiments is defined as the observed difference between a calculated and measured response. In conventional validation studies, such as those using USLSTATS, the expected bias in an application response (for which there is no measurement, by definition) often is estimated as the sample mean of the biases for a set of benchmark experiments, and the uncertainty in the application bias is estimated by the sample standard deviation of the experimental biases.

The GLLS technique provides another method to compute the bias of an application response. The application response bias $\beta_a$ is defined as the expected deviation of the original calculated response $k_a$ from the best estimate of the measured response, which is unknown but has some probability distribution. Note that if the application response actually did have a prior measured value $m_a$, then the best estimate for the application value would be the final adjusted value $m'_a$ obtained from the GLLS procedure. For this reason the notation $m'_a$ is used here to represent the (unknown) best estimate for the application's projected measured response, so that

$$\beta_a = E[k_a - m'_a] \ , \tag{11}$$

where $E[\cdot]$ is the expectation operator. The application's projected measured value can be expressed as $m'_a = k_a(\boldsymbol{\alpha}') - \delta m_a$, where $\delta m_a$ represents the difference between the best-computed response obtained with the adjusted data $\boldsymbol{\alpha}'$ and the expected value of the actual measurement. Therefore, Eq. (11) can be expressed as

$$\begin{aligned}\beta_a &= E[k_a - k_a(\boldsymbol{\alpha}') + \delta m_a] \\ &= k_a - k_a(\boldsymbol{\alpha}') + E[\delta m_a] \ .\end{aligned} \tag{12}$$

Recall that all experiment responses are sure to have $\delta m_i = 0$ because the GLLS procedure forces $k' = m'$ within the approximation of first-order theory. However, $\delta m_a$ $(= k_a - m'_a)$ for the application is not guaranteed to be zero since there is no known measured value. Nevertheless, the application response calculated using the best cross sections $\boldsymbol{\alpha}'$ should approach the desired (unknown) measured value if a sufficient number of experiments similar to the application of interest are considered so that under these conditions $E[\delta m_a] \rightarrow 0$ for the application as well.[9] More details concerning the suitable degree of similarity and the sufficient number of experiments necessary for convergence of the GLLSM are discussed in other publications.[9]

Assuming an adequate benchmark database, we simplify Eq. (12) to

$$\beta_a = k_a - k_a(\boldsymbol{\alpha}') \approx -(k_a)\mathbf{S}_a^T \Delta\boldsymbol{\alpha} \ , \tag{13}$$

where

$\mathbf{S}_a$ = vector of the groupwise $S_j$ for all nuclide reactions

$\Delta\boldsymbol{\alpha}$ = vector of adjustments to the cross sections.

### *III.B. Bias Uncertainty*

In most cases some gaps exist in the benchmark database so that $E[\delta m_a] \neq 0$. In this case, the adjusted cross-section-covariance data $\mathbf{C}_{\boldsymbol{\alpha}'\boldsymbol{\alpha}'}$ are used to produce a postadjustment uncertainty, which is the uncertainty in the adjusted response value and, thus, the uncertainty in the computational bias. The postadjustment uncertainty for the application is computed as

$$\sigma_{k_a}^2 = \mathbf{S}_a \mathbf{C}_{\boldsymbol{\alpha}'\boldsymbol{\alpha}'} \mathbf{S}_a^T \ , \tag{14}$$

and the uncertainty in the bias is

$$\Delta\beta_a = \sqrt{\mathbf{S}_a \mathbf{C}_{\boldsymbol{\alpha}'\boldsymbol{\alpha}'} \mathbf{S}_a^T} \ . \tag{15}$$

The individual nuclide-reaction-specific contributors to the bias uncertainty can be computed from the individual processes that make up the postadjustment cross-section-covariance data. When folded with the application sensitivity data for the same processes, gaps in the benchmark database that contribute to the uncertainty in the bias are revealed.

### *III.C. Bias Assessment with TSURFER Using $k_{eff}$ Reactivity Sensitivity Data*

When extracting the bias for a single material from an integral benchmark experiment, one may find it difficult to examine a single experiment and differentiate bias due to a test material from bias due to other materials such as fuel and moderator. An alternative method is to examine two experiments from the same critical assembly—one with the test material and one without it—and examine differences in the biases due to the introduction of the test material. TSURFER can provide only high-quality biases with low uncertainties where appropriate experimental data are available. For replacement measurements for test materials, such as the FPs, it is advantageous to employ a means of emphasizing the test material through the use of two highly correlated experiments—one with the test material and one without it. Since both experiments are critical, the change in $k_{eff}$ between the two systems (the reactivity difference) would be zero, within experimental uncertainties. However, if there were a computational bias due to the test material, the computed reactivity between the two experiments would not be zero, as the experiment with the test material would have a different computational bias from the experiment without the test material. This replacement technique magnifies the effect of the test material because all other materials are nearly the same, and sources of uncertainty between the two experiments are highly correlated. The primary source of bias difference between the two measurements is the test material itself.

To quantify the measured bias for the test material, we generated TSUNAMI $k_{eff}$ sensitivity data for each experiment in a pair and applied TSAR to determine the sensitivity of the reactivity between the two systems to the cross-section data. TSAR determines on a nuclide-reaction and energy-dependent basis the sensitivity of changes in computed $k_{eff}$ between two systems to the cross-section data. Thus, if the primary difference between two critical measurements is the test material, TSAR determines, on an energy-dependent basis, how sensitive the bias is to the test material. TSURFER then determines the sources of bias, using not only $k_{eff}$ sensitivity data but also reactivity sensitivity data. For the test material, TSURFER applies its data adjustment procedure to obtain a consistency between the measured reactivity difference (zero for two critical experiments) and calculated reactivity difference (likely not zero) for each of one or more pairs of systems, determining the best-estimate cross-section adjustments for the test material. The observed partial bias due to the test material is then projected to a bias in the application by multiplying the cross-section adjustments that eliminate the bias in the experiments by the application's $k_{eff}$ sensitivity coefficients for the same material. This product gives the relative bias in the application's computed $k_{eff}$ value due to the test material.

For the analyses below, TSURFER and TSAR are employed as follows. To use the observed bias due to the test material, in this case a FP, we generate TSUNAMI $k_{eff}$ sensitivities for each pair of experiments and apply TSAR to determine the sensitivity of the reactivity between the two systems to the cross-section data. TSAR determines on a nuclide-reaction and energy-dependent basis the sensitivity of the changes in computed $k_{eff}$ between the two systems to the cross-section data. Consequently, if the primary difference between two critical

measurements is the FP, TSAR determines how sensitive the bias is to the FP.

For a given NFP/FP experiment pair, several experiments are included as experiment $k_{eff}$ responses, which means they are included in the adjustment process and hence impact the data. In addition, the reactivity-difference response (with sensitivities from TSAR) is also included as an experiment response. The FP experiment is included as an application response, which means that it does not impact the adjustment procedure but its own response is adjusted.

Because the reactivity difference is relatively insensitive to all but the FP nuclides, that response does not significantly impact the adjustment of the other nuclide cross sections. However, the reactivity-difference response does lead to adjustment of the FP cross sections. This adjustment, when propagated to the FP experiment, is the FP partial bias in the FP experiment. Moreover, the same FP cross-section changes can be propagated to the (true) application system, leading to the partial bias of interest. Subsequently, the weighting methods of Sec. IV can be used to develop an application FP bias using FP biases derived from several experiment pairs.

It should be noted that the method by which TSURFER is used here is similar to but distinct from recent related work.[10]

### *III.D. Detailed Bias and Bias Uncertainty Assessment with TSURFER*

A unique feature of TSURFER is the ability to provide a detailed assessment of sources of the computational bias. By multiplying element-wise the application sensitivity $\mathbf{S}_a$ with the cross-section changes $\Delta\boldsymbol{\alpha}$, and multiplying the result by $-1$, a vector of groupwise biases for all nuclide reactions is produced. The energy dependence of the bias reflects the energy-dependent structure of the sensitivity data as well the shape of the data adjustments. Additionally, the uncertainty in the bias can be viewed according to its contributions from the adjusted cross-section covariance matrices.

## IV. COMBINING APPLICATION PARTIAL BIASES

Section III details a method to extract partial biases from experiments and to propagate the associated cross-section changes to the application system of interest. Recent work has outlined a method by which an application partial bias can be computed from several individual experiments simultaneously using TSURFER (Ref. 10). In that approach, several experiments are used together in a single adjustment to produce a partial bias for the application system. Here, we offer an alternative scheme that weights and sums application biases computed from individual experiments to form an effective application bias. The methodology described here is an adaptation of recent work.[11]

### *IV.A. Penalty due to Dissimilarity*

We noted above that Eq. (10) does not provide a proper penalty for dissimilarities between two sensitivity profiles. Here, a proper expression for that penalty is derived for subsequent use in combining biases and as another metric of similarity. Other work has also applied this penalty directly to subcritical limits and used a different definition for bias uncertainty than is used below.[11] The application bias defined in this section is only used in the construction of the penalty as full energy-dependent biases from TSURFER are used in subsequent analysis.

Recall that the $k_{eff}$ sensitivity to perturbations in cross-section data is defined by

$$S_j = \frac{\Delta k_j / k}{\Delta\sigma_j / \sigma_j} \rightarrow \frac{\Delta k_j}{k S_j} = \frac{\Delta\sigma_j}{\sigma_j} \quad . \tag{16}$$

If the same cross-section data are used for both an application and experiment system, Eq. (16) can be written

$$\frac{\Delta k_{a,j}}{k_a S_{a,j}} = \frac{\Delta\sigma_j}{\sigma_j} = \frac{\Delta k_{e,j}}{k_e S_{e,j}} \quad , \tag{17}$$

and solving for $\Delta k_{a,j}$ yields

$$\Delta k_{a,j} = \frac{S_{a,j}}{S_{e,j}} \times \frac{k_a}{k_e} \times \Delta k_{e,j} \quad , \tag{18}$$

where the $\Delta k_j$ represent groupwise biases. Were such groupwise biases known (e.g., from TSURFER), then the total application bias $\beta_a$ can be defined as

$$\beta_a = \sum_j \Delta k_{a,j} = \frac{k_a}{k_e} \times \sum_j \left( \frac{S_{a,j}}{S_{e,j}} \times \Delta k_{e,j} \right) \quad . \tag{19}$$

If $S_{a,j}$ and $S_{e,j}$ are exactly the same qualitatively (i.e., they are proportional for all $j$), then,

$$\begin{aligned} \beta_a &= \frac{k_a}{k_e} \times \frac{S_a}{S_e} \times \beta_e \\ &= \frac{k_a}{k_e} \times \frac{1}{\lambda} \times \beta_e \quad , \end{aligned} \tag{20}$$

where $\lambda = \sum_j S_{e,j} / \sum_j S_{a,j} = S_e / S_a$, $S_a$ and $S_e$ represent energy-integrated sensitivities and where we define the experiment bias to be $\sum_j \Delta k_{e,j} = \beta_e$, which is not yet explicitly known since $\beta_e$ represents a partial bias and only a total bias is known a priori. The interpretation of Eq. (20) is clear: It defines the application partial bias as simply a normalization of the experiment bias by the integrated application sensitivity and response.

In general, $S_{a,j}$ and $S_{e,j}$ are not proportional for all $j$. To account for "dissimilarity" between the sensitivity profiles, we rewrite Eq. (19) as

$$\beta_a = \frac{k_a}{k_e} \times \sum_j \left( \frac{S_{a,j}}{\lambda(S_{a,j} - \hat{Z}_j)} \times \Delta k_{e,j} \right) , \tag{21}$$

where $\hat{Z}_j = S_{a,j} - S_{e,j}/\lambda$; we recognize $\hat{Z}_j$ from the definition of $p_{\hat{g}}$ defined in Eq. (10). For $\hat{Z}_j \ll S_{a,j}$, Eq. (21) simplifies to

$$\beta_a = \frac{k_a}{\lambda k_e} \beta_e + \frac{k_a}{\lambda k_e} \sum_j \left( \frac{\hat{Z}_j}{S_{a,j}} \times \Delta k_{e,j} \right) . \tag{22}$$

The second term of Eq. (22) in effect is the "error" due to dissimilarity between the profiles. Of course, from TSURFER, one can readily obtain values for $\Delta k_{e,j}$ in Eq. (22). However, one can also use bounding estimates for the groupwise biases. Any computational bias is assumed to be due only to errors in the nuclear data, and so the groupwise biases can be approximated as

$$\Delta k_{e,j} \approx k_e \times S_{e,j} \times \frac{\Delta\sigma_j}{\sigma_j} , \tag{23}$$

where $\Delta\sigma_j/\sigma_j$ represents the relative groupwise cross-section uncertainty. Using this expression, we can rewrite the second term of Eq. (22) as

$$p_{ds} = \frac{k_a}{\lambda} \sum_j \left( \frac{S_{e,j}\hat{Z}_j}{S_{a,j}} \frac{\Delta\sigma_j}{\sigma_j} \right) , \tag{24}$$

where $p_{ds}$ denotes a penalty due to dissimilarity. Defining $Z_j = S_{e,j}\hat{Z}_j/S_{a,j}$, we have Eq. (24) becoming

$$p_{ds} = \frac{k_a}{\lambda} \sum_j \left( Z_j \frac{\Delta\sigma_j}{\sigma_j} \right) . \tag{25}$$

While $Z_j$ can be either positive or negative, the relative uncertainty in the cross-section data can be in either direction. Thus, the conservative approach is to let the resulting error always add to the bias. Hence,

$$\beta_a = \frac{k_a}{\lambda k_e} \beta_e + \frac{k_a}{\lambda} \sum_j \left| Z_j \frac{\Delta\sigma_j}{\sigma_j} \right| . \tag{26}$$

Using standard matrix notation for the cross-section uncertainty, which also correctly incorporates the covariance terms, yields

$$\begin{aligned} p_{ds} &= \frac{k_a}{\lambda} \sqrt{\mathbf{Z}\mathbf{C}_{\sigma\sigma}\mathbf{Z}^T} \\ &= \frac{S_a k_a}{S_e} \sqrt{\mathbf{Z}\mathbf{C}_{\sigma\sigma}\mathbf{Z}^T} , \end{aligned} \tag{27}$$

where $T$ denotes the matrix transpose. Equation (27) defines the proper penalty for dissimilarity [compare to Eq. (9)]. Note that $p_{ds}$ is used here only as a means to weight individual biases (as in Sec. IV.A.1) and not as a penalty applied to the biases computed.

### IV.A.1. Combining Single Biases

Further, a method for combining several partial biases is developed. The aim is to combine several application biases found via the method of Sec. III.

For the case of $N$ experiments, each yielding an application bias $\beta_i^a$ and penalty $p_{ds}$, a method to combine all $N$ experiments is needed. Let an effective application bias be defined $\beta_a = \sum_i^N w_i \beta_a^i$, where the $w_i$ are weights subject to $\sum_i w_i = 1$ and $w_i \geq 0$.

There are at least two basic approaches for finding such weights. One method would be to weight experiments based solely on their qualitative similarity to the application using the sensitivity data. A parameter already exists for quantifying such similarity, namely, $\hat{g}$. A weighting scheme using this parameter could be defined by letting

$$w_i = \frac{\hat{g}_i}{\sum_j^N \hat{g}_j} , \tag{28}$$

where only experiments with $g_i > 0$ are included.

A second scheme would be to minimize the penalty due to dissimilarity, i.e., the sum of the $p_{ds}$ terms. Because these terms quantify an estimated uncertainty, it is necessary to add them in quadrature. Therefore, the goal becomes to minimize the quantity

$$\begin{aligned} &\left( w_1 \frac{k_a S_a}{S_{e1}} \sqrt{\mathbf{Z}_1 \mathbf{C}_{\sigma\sigma} \mathbf{Z}_1^T} \right)^2 + \left( w_2 \frac{k_a S_a}{S_{e2}} \sqrt{\mathbf{Z}_2 \mathbf{C}_{\sigma\sigma} \mathbf{Z}_2^T} \right)^2 + \ldots \\ &\quad = w_1^2 \left( \frac{k_a S_a}{S_{e1}} \right)^2 \mathbf{Z}_1 \mathbf{C}_{\sigma\sigma} \mathbf{Z}_1^T + w_2^2 \left( \frac{k_a S_a}{S_{e2}} \right)^2 \mathbf{Z}_2 \mathbf{C}_{\sigma\sigma} \mathbf{Z}_2^T \\ &\qquad + \ldots \\ &\quad = \sum_{i=1}^N w_i^2 p_{ds,i}^2 . \end{aligned} \tag{29}$$

Because the minimization must also satisfy the weight constraint, $\sum_i^N w_i = 1$ and $w_i \geq 0$ for all $i$, the problem can be written

$$\begin{aligned} \text{min} \quad & P = w_1^2 p_{ds,1}^2 + w_2^2 p_{ds,2}^2 + \cdots + w_N^2 p_{ds,N}^2 \\ \text{subject to} \quad & w_1 + w_2 + \cdots + w_N = 1 \\ & w_i \geq 0 . \end{aligned} \tag{30}$$

This is a quadratic program, which can be transformed into an equivalent linear complementarity problem and solved via the Lemke's method.[12]

## V. EXAMPLE ANALYSES

In this section, the methods described in Secs. III and IV are applied to two series of critical experiments that investigated FPs relevant to burnup credit. The experiments are included in the *International Handbook of Evaluated Criticality Safety Benchmark Experiments*[13] (IHECSBE). All computations were performed using SCALE 6 and its ENDF-VI.8 238-group-cross-section library.

### *V.A. Fission Product Replacement-Worth Experiments*

The LEU-COMP-THERM (LCT)-050 (LCT-050) experiment was performed in France and investigated $^{149}$Sm. The experiments consisted of aluminum-clad $UO_2$ (4.738% enriched) rods situated about a central Zircaloy tank. For two configurations, the tank was filled with slightly acidic water. Five configurations used boron solutions, and the final 11 used samarium solution (enriched in $^{149}$Sm).

The fuel rods were arranged in a 1.3-cm square-pitched array and were water moderated. Several cases used the same boron or samarium concentration but with different numbers of fuel rods. The approach to critical was done via adjusting the water height. Table I summarizes the individual cases. Note that case LCT-050-001 is used as the NFP reference case for the FP cases analyzed.

TABLE I

Summary of LCT-050 Cases

| Case Number | Identifier | Description |
|---|---|---|
| 1 | LCT-050-001 | Acidic water |
| 2 | LCT-050-002 | Acidic water |
| 3 | LCT-050-003 | Boron (0.822 g/ℓ) |
| 4 | LCT-050-004 | Boron (0.822 g/ℓ) |
| 5 | LCT-050-005 | Boron (0.822 g/ℓ) |
| 6 | LCT-050-006 | Boron (5.03 g/ℓ) |
| 7 | LCT-050-007 | Boron (5.03 g/ℓ) |
| 8 | LCT-050-008 | Samarium (0.1048 g/ℓ) |
| 9 | LCT-050-009 | Samarium (0.1048 g/ℓ) |
| 10 | LCT-050-010 | Samarium (0.1048 g/ℓ) |
| 11 | LCT-050-011 | Samarium (0.2148 g/ℓ) |
| 12 | LCT-050-012 | Samarium (0.2148 g/ℓ) |
| 13 | LCT-050-013 | Samarium (0.2148 g/ℓ) |
| 14 | LCT-050-014 | Samarium (0.6262 g/ℓ) |
| 15 | LCT-050-015 | Samarium (0.6262 g/ℓ) |
| 16 | LCT-050-016 | Samarium (0.6262 g/ℓ) |
| 17 | LCT-050-017 | Samarium (0.6262 g/ℓ) |
| 18 | LCT-050-018 | Samarium (0.6262 g/ℓ) |

TABLE II

Summary of LCT-079 Cases

| Case Number | Identifier | Description |
|---|---|---|
| 1 | LCT-079-001 | 2.0-cm pitch; NFP; normal fuel rods throughout |
| 2 | LCT-079-002 | 2.0-cm pitch; NFP; experimental rods without foils |
| 3 | LCT-079-003 | 2.0-cm pitch; 25-$\mu$m rhodium foils |
| 4 | LCT-079-004 | 2.0-cm pitch; 50-$\mu$m rhodium foils |
| 5 | LCT-079-005 | 2.0-cm pitch; 100-$\mu$m rhodium foils |
| 6 | LCT-079-006 | 2.8-cm pitch; NFP; normal fuel rods throughout |
| 7 | LCT-079-007 | 2.8-cm pitch; NFP; experimental rods without foils |
| 8 | LCT-079-008 | 2.8-cm pitch; 25-$\mu$m rhodium foils |
| 9 | LCT-079-009 | 2.8-cm pitch; 50-$\mu$m rhodium foils |
| 10 | LCT-079-010 | 2.8-cm pitch; 100-$\mu$m rhodium foils |

The LCT-079 experiment, performed at Sandia National Laboratories, investigated $^{103}$Rh. This experiment consisted of rhodium foils placed between fuel pellets in several rods at the center of a hexagonal array of $UO_2$ rods (4.382% enriched) in water. Ten individual experiments were performed. Half of the experiments (five) used a 2.0-cm pitch, producing moderation representative of typical light water reactors. The other five experiments used a 2.8-cm pitch, which yielded optimal moderation.

For each subset of five, two reference (NFP) experiments were performed. The first of these used normal fuel rods throughout. The second used the experimental rods without rhodium foils in place. The experiment rods were very similar to the normal rods except for small gaps between fuel pellets for placing foils. The final three used rhodium foils of 25-, 50-, and 100-$\mu$m thickness, respectively. The approach to critical was done via adding fuel rods. Table II summarizes the individual cases. Note that cases LCT-079-002 and LCT-079-007 are used as the NFP references for the 2.0- and 2.8-cm pitch cases, respectively.

Table III summarizes the benchmark model and computed $k_{eff}$, $\rho$, and uncertainties for each experiment used in the analyses below. The reactivity is reported in units of percent-milli (pcm) or $10^{-5}$ $\Delta k$. The uncertainty in the $\rho_m$'s was computing by assuming a correlation coefficient of $C_{\mathrm{FP/NFP}} = 0.98$ and using the standard formula:

$$\sigma_{\rho_m} = \sqrt{\sigma_{k_{\mathrm{NFP}}}^2 - \sigma_{k_{\mathrm{FP}}}^2 - 2C_{\mathrm{FP/NFP}}\sigma_{k_{\mathrm{NFP}}}\sigma_{k_{\mathrm{FP}}}} \ , \qquad (31)$$

where FP and NFP denote the cases with and without the FP.

TABLE III

Summary of LCT-050 and LCT-079 Measured and Calculated $k_{eff}$, $\rho$, and Uncertainties

| Identifier | $k_{eff}$ (Measured) | $\sigma_k$ | $\rho$ (Measured) (pcm) | $\sigma_{\rho_m}$ | $k_{eff}$ (Calculated) | $\sigma_k$ | $\rho$ (Calculated) (pcm) | $\sigma_{\rho_c}$ |
|---|---|---|---|---|---|---|---|---|
| LCT-050-001 | 1.0004 | 0.0010 | — | — | 0.99056 | 0.00020 | — | — |
| LCT-050-008 | 1.0004 | 0.0010 | 0 | 20 | 0.98796 | 0.00020 | 266 | 28 |
| LCT-050-012 | 1.0004 | 0.0010 | 0 | 20 | 0.98979 | 0.00020 | 79 | 28 |
| LCT-050-013 | 1.0004 | 0.0010 | 0 | 20 | 0.98994 | 0.00018 | 64 | 27 |
| LCT-050-014 | 1.0004 | 0.0010 | 0 | 20 | 0.98987 | 0.00020 | 71 | 28 |
| LCT-050-015 | 1.0004 | 0.0010 | 0 | 20 | 0.99041 | 0.00020 | 16 | 28 |
| LCT-050-016 | 1.0004 | 0.0010 | 0 | 20 | 0.99153 | 0.00020 | −98 | 28 |
| LCT-050-017 | 1.0004 | 0.0010 | 0 | 20 | 0.99146 | 0.00020 | −91 | 28 |
| LCT-050-018 | 1.0004 | 0.0010 | 0 | 20 | 0.99155 | 0.00020 | −100 | 28 |
| LCT-079-002 | 1.0002 | 0.0016 | — | — | 0.9897 | 0.0002 | — | — |
| LCT-079-003 | 1.0005 | 0.0016 | −30 | 32 | 0.9901 | 0.0002 | −39 | 28 |
| LCT-079-004 | 1.0004 | 0.0016 | −20 | 32 | 0.9904 | 0.0002 | −66 | 28 |
| LCT-079-005 | 1.0004 | 0.0016 | −20 | 32 | 0.9906 | 0.0002 | −87 | 28 |
| LCT-079-007 | 1.0003 | 0.0008 | — | — | 0.9932 | 0.0002 | — | — |
| LCT-079-008 | 1.0008 | 0.0008 | −50 | 16 | 0.9944 | 0.0002 | −120 | 28 |
| LCT-079-009 | 1.0003 | 0.0008 | 0 | 16 | 0.9941 | 0.0002 | −97 | 28 |
| LCT-079-010 | 1.0009 | 0.0008 | −60 | 16 | 0.9950 | 0.0002 | −185 | 28 |

### *V.B. Demonstration Application System*

The application system used for this analysis is the Transportation, Aging, and Disposal (TAD) canister-based system.[14] The TAD canister is designed to hold 21 pressurized water reactor used fuel assemblies limited to <5% initial enrichment, <80 GWd/tonne U burnup, and at least 5 yr out-of-reactor cooling time.

The TAD canister consists of an external corrosion-resistent Alloy 22 vessel [5.08-cm (2-in.) wall thickness], an intermediate steel vessel [5.08-cm (2-in.) wall thickness], and an internal steel vessel [2.54-cm (1-in.) top and side thickness; 8.89-cm (3.5-in.) bottom thickness]. The basket consists of square stainless steel tubes with 0.6-cm (0.2362-in.) boronated steel absorbers between assemblies and on the outside faces of the peripheral assemblies. The TAD canister is modeled with a Dry Tuff surrounding at 27°C (80.6°F).

For this work, the TAD canister is modeled as fully flooded with full-density water and loaded with 21 Babcock and Wilcox 15 × 15 assemblies burned to 40 GWd/tonne U, with 5-yr cooling and a 5% initial enrichment. This configuration was the most reactive state studied by ORNL for the particular burnup.

The STARBUCS sequence of SCALE was used to generate burned fuel compositions in seven axial regions. The following nuclides were retained for the following analyses: $^{16}$O, $^{95}$Mo, $^{99}$Tc, $^{99}$Ru, $^{103}$Rh, $^{109}$Ag, $^{143}$Nd, $^{145}$Nd, $^{147}$Sm, $^{149}$Sm, $^{150}$Sm, $^{151}$Sm, $^{152}$Sm, $^{151}$Eu, $^{153}$Eu, $^{155}$Gd, $^{233}$U, $^{234}$U, $^{235}$U, $^{236}$U, $^{238}$U, $^{237}$Np, $^{238}$Pu, $^{239}$Pu, $^{240}$Pu, $^{241}$Pu, $^{242}$Pu, $^{241}$Am, $^{242m}$Am, and $^{243}$Am. The computed $k_{eff}$ is 0.959874 ± 0.000214.

### *V.C. Similarity*

Before one computes partial FP biases for application to the TAD model, it is instructive to assess how similar to the TAD canister the LCT-050 and LCT-079 experiments are with respect to $^{149}$Sm and $^{103}$Rh, respectively. Here, only the $(n,\gamma)$ reaction is used for both nuclides in comparisons, as the corresponding sensitivities for this reaction are several orders of magnitude larger than for other reactions. It is possible to assess such similarity both visually and via use of indices like $\hat{g}$ from Sec. II as well as $g$ and individual (nuclide-specific) $c_k$ values from TSUNAMI-IP.

Figure 1 depicts the sensitivity profiles with associated $\hat{g}$ values for a number of LCT-050 and LCT-079 cases with the associated TAD canister profiles. The LCT-079 profiles, and in particular LCT-079-005, exhibit rather poor qualitative fits due to the high self-shielding of the foil used.

Additionally, Table IV lists the $\hat{g}$, $p_{ds}$, $g$, and individual $c_k$ values for each of the experiments. The LCT-050 cases all show moderately good similarity to the TAD canister using $\hat{g}$, $g$, and individual $c_k$. The individual $c_k$ values are equal to unity to three decimals. Moreover, for all but one case, $g > 0.9$, which indicates a high degree of coverage. The $\hat{g}$ values are slightly lower, which indicates that while the experiments are at least as

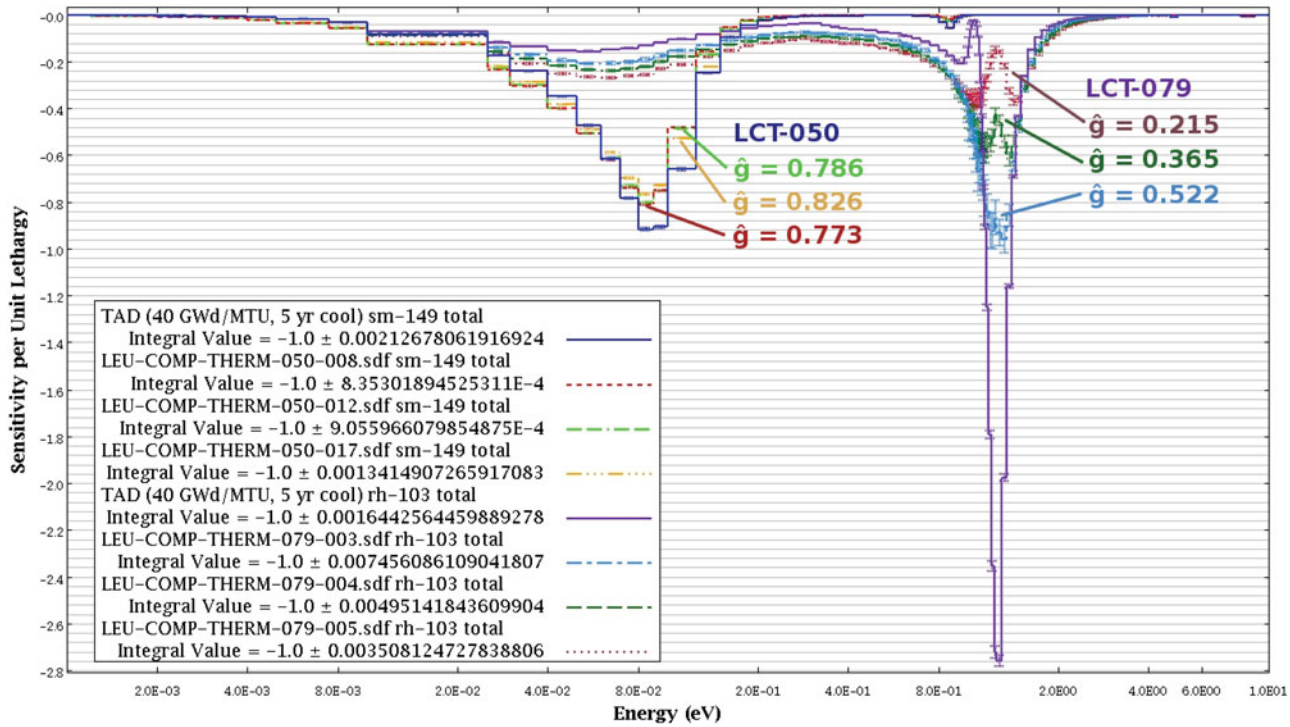


Fig. 1. The $\hat{g}$ values for several LCT-050 and LCT-079 cases. Note that all sensitivity profiles are normalized to negative unity for comparison.

TABLE IV

Summary of LCT-050 and LCT-079 Partial Biases, Associated TAD Canister Bias, and Qualitative Parameters*

| Identifier | $\beta_e$ | $\Delta\beta_e$ | $\beta_a$ | $\Delta\beta_a$ | $\hat{g}$ | $g$ | Individual $c_k$ | $p_{ds}$ |
|---|---|---|---|---|---|---|---|---|
| LCT-50-008 | −140.63 | 15.97 | −134.22 | 15.32 | 0.773 | 0.891 | 1.000 | 5.593 |
| LCT-50-012 | −75.66 | 19.84 | −56.17 | 14.79 | 0.786 | 0.979 | 1.000 | 5.332 |
| LCT-50-013 | −71.52 | 19.65 | −53.46 | 14.75 | 0.788 | 0.980 | 1.000 | 5.281 |
| LCT-50-014 | −58.19 | 19.76 | −49.82 | 16.96 | 0.827 | 0.972 | 1.000 | 4.359 |
| LCT-50-015 | −41.63 | 20.23 | −34.74 | 16.93 | 0.821 | 0.978 | 1.000 | 4.520 |
| LCT-50-016 | 5.26 | 19.85 | 4.46 | 16.9 | 0.816 | 0.970 | 1.000 | 4.649 |
| LCT-50-017 | 2.34 | 19.92 | 1.97 | 16.82 | 0.826 | 0.977 | 1.000 | 4.383 |
| LCT-50-018 | 4.37 | 19.62 | 3.78 | 17.01 | 0.829 | 0.969 | 1.000 | 4.302 |
| LCT-79-003 | −0.12 | 4.51 | −0.71 | 24.97 | 0.522 | 0.205 | 0.995 | 10.841 |
| LCT-79-004 | 1.96 | 13.77 | 3.38 | 23.14 | 0.365 | 0.652 | 0.983 | 11.666 |
| LCT-79-005 | 6.65 | 22.25 | 5.7 | 20.06 | 0.215 | 0.676 | 0.952 | 11.342 |
| LCT-79-008 | 41.17 | 5.34 | 21.12 | 24.22 | 0.306 | 0.378 | 0.938 | 8.736 |
| LCT-79-009 | 4.41 | 13.73 | 19.56 | 20.07 | 0.204 | 0.665 | 0.880 | 8.984 |
| LCT-79-010 | 31.65 | 23.29 | 38.56 | 19.42 | 0.109 | 0.684 | 0.783 | 9.617 |

*The $\beta$'s, $\Delta\beta$'s, and $p_{ds}$ are in units of pcm.

sensitive to the TAD canister for $^{149}$Sm over most energy groups (i.e., a high $g$), the energy dependences are not proportional. For the LCT-079 series, only cases LCT-79-009 and LCT-79-010 have individual $c_k$ values that are below 0.9. On the other hand, both $g$ and $\hat{g}$ are quite low for all the experiments, which means that the experiment sensitivities are neither at least as large as the TAD canister sensitivity over many groups nor exhibit an energy dependence similar to that of the TAD canister sensitivity.

### *V.D. Bias Determination*

As described above, even with TSURFER, it can be difficult if not impossible to distinguish bias contributions in a single experiment due to a low-impact test material from more important materials such as the fuel or moderator. A way to circumvent this issue is to consider two experiments from the same series—one with the test material and one without it—and to analyze the bias in the reactivity difference between the two experiments. If the experiments are identical except for that test material, the bias should be due only to the test material. In this case, both the LCT-050 and LCT-079 are $UO_2$ experiments, and so, a set of similar $UO_2$ experiments is required to isolate the partial bias due to $^{149}$Sm and $^{103}$Rh, respectively.

#### V.D.1. $UO_2$ Experiments for the Adjustment

For this analysis, 54 experiments from IHECSBE were selected for inclusion in the adjustment procedure to account for NFP nuclides; these came from evaluations LEU-COMP-THERM-010, -017, -026, -042, and -049. Certainly, many more potentially useful experiments exist, but these were the cases for which SCALE 6 TSUNAMI-3D-K5 sensitivity data using ENDF/B-VI.8 cross sections were available at the time of this work.

Table V lists each experiment, its measured and calculated $k_{eff}$, and the index $c_k$ with respect to each of the reference NFP cases. Only LCT-049-001, -002, and -003 had $c_k < 0.8$ for all three reference cases, and 12 of the LCT-049 series had $c_k < 0.8$ for the reference case LCT-079-007. This is expected as LCT-079-007 is optimally moderated and, consequently, has a softer spectrum than the likely undermoderated LCT-049 series. Of the 54 experiments, 26, 23, and 16 had $c_k \geq 0.9$ for LCT-050-001, LCT-079-002, and LCT-079-007, respectively. At least for the first two reference cases, a high degree of coverage is expected. Previous work has suggested that at least 15 experiments with $c_k \geq 0.9$ are needed for a bias to be "converged."[9]

TSURFER allows the user to input the correlations between individual experiment uncertainties. This is useful if, for example, experiments are from the same series and use the same assembly. For the following analyses, all within-series experiments were assumed to have a correlation of 0.8, and all experiments not in the same series were assumed to be uncorrelated. Determining the exact correlation of experiments is a difficult task, largely because of a lack of available information. The effect of the interseries correlation on bias is examined briefly in Sec. VI.

Note that the $\chi^2$ filter value of TSURFER was set high so that no experiments (and, in particular, the reactivity-difference response) were left out of the adjustment. Generally, this would be inadvisable, but for this demonstration process, it was necessary in order to keep the desired response included without resorting to somewhat manual filtering.

#### V.D.2. Partial Biases

The partial biases corresponding to the FP experiments described above were determined using TSURFER, the $UO_2$ experiments, and the eigenvalue-difference sensitivities for the various experiment pairs. Additionally, the corresponding cross-section adjustments were propagated to the TAD canister via sensitivities to produce the application partial biases. Table IV provides a summary of the individual partial biases ($\beta$) for both the FP experiments and the TAD canister as well as qualitative parameters computed for the FP experiments.

The uncertainty in the partial biases is defined as above to be the sensitivity folded with the adjusted covariance data, i.e., $\Delta\beta = \sqrt{\mathbf{S}_k \mathbf{C}_{\alpha'\alpha'} \mathbf{S}_k^T}$. Here, $\mathbf{S}_k$ and $\mathbf{C}_{\alpha'\alpha'}$ are for only the FP nuclide of interest.

From the individual partial biases, appropriate partial biases were determined for the TAD canister. These biases, along with associated uncertainties, are provided in Table VI. Additionally, a bounding estimate for the biases denoted is included, which is simply the application sensitivity for the nuclide folded with the original covariance data for the specific nuclide. Previous research suggests that the application uncertainty in $k_{eff}$ computed in this manner is a 1-$\sigma$ bound on the true bias.[5] For $^{103}$Rh, the total bias computed including the uncertainty is slightly less than the 1-$\sigma$ estimated bound. For $^{149}$Sm, the bias is just less than the 2-$\sigma$ estimate; this is high and is most likely due to the high correlation assumed (see below). Note that the $^{149}$Sm bias is negative, which means that its worth is underestimated and that the magnitude of the bias should be subtracted from the upper subcritical limit.

## VI. CORRELATIONS IN BENCHMARK UNCERTAINTIES

The IHECSBE provides extensive documentation on benchmark uncertainties for individual experiments, and previous research has demonstrated a methodology to generate correlations in uncertainties between benchmarks.[15] The IHECSBE includes some data documenting experimental correlation in the DICE database included in the DVD distribution. However, the data available represent only a few dozen of the more than 4000 benchmark configurations documented in IHECSBE.

The partial biases for $^{103}$Rh and $^{149}$Sm listed in Table IV were determined using a set number of experiments in addition to several assumptions regarding experimental uncertainties and correlations. The idea was merely to provide a somewhat realistic example of the methods developed in Secs. III and IV.

TABLE V

Specification of $UO_2$ Benchmark Experiments

| Case Number | Identifier | $k_{eff}$ (Calculated) | $\sigma_{k(c)}$ | $k_{eff}$ (Measured) | $\sigma_{k(m)}$ | $\frac{m}{c} - 1$ (%) | $c_k$ [a] | $c_k$ [b] | $c_k$ [c] |
|---|---|---|---|---|---|---|---|---|---|
| 1 | LCT-010-005 | 0.99505 | 0.0002 | 1.0000 | 0.0018 | 0.50 | 0.915 | 0.892 | 0.921 |
| 2 | LCT-010-016 | 0.99362 | 0.0002 | 1.0000 | 0.0026 | 0.64 | 0.978 | 0.980 | 0.948 |
| 3 | LCT-010-017 | 0.99370 | 0.0002 | 1.0000 | 0.0026 | 0.63 | 0.980 | 0.982 | 0.951 |
| 4 | LCT-010-018 | 0.99244 | 0.0002 | 1.0000 | 0.0026 | 0.76 | 0.981 | 0.983 | 0.952 |
| 5 | LCT-010-019 | 0.99172 | 0.0002 | 1.0000 | 0.0026 | 0.83 | 0.986 | 0.988 | 0.957 |
| 6 | LCT-017-003 | 0.99271 | 0.0002 | 1.0000 | 0.0030 | 0.73 | 0.932 | 0.911 | 0.933 |
| 7 | LCT-017-004 | 0.99187 | 0.0002 | 1.0000 | 0.0030 | 0.82 | 0.867 | 0.846 | 0.869 |
| 8 | LCT-017-005 | 0.99450 | 0.0002 | 1.0000 | 0.0030 | 0.55 | 0.887 | 0.865 | 0.890 |
| 9 | LCT-017-006 | 0.99387 | 0.0002 | 1.0000 | 0.0030 | 0.62 | 0.895 | 0.873 | 0.899 |
| 10 | LCT-017-007 | 0.99372 | 0.0002 | 1.0000 | 0.0030 | 0.63 | 0.901 | 0.879 | 0.905 |
| 11 | LCT-017-008 | 0.99207 | 0.0002 | 1.0000 | 0.0030 | 0.80 | 0.912 | 0.888 | 0.917 |
| 12 | LCT-017-009 | 0.99032 | 0.0002 | 1.0000 | 0.0030 | 0.98 | 0.935 | 0.913 | 0.938 |
| 13 | LCT-017-010 | 0.99252 | 0.0002 | 1.0000 | 0.0030 | 0.75 | 0.913 | 0.893 | 0.912 |
| 14 | LCT-017-011 | 0.99287 | 0.0002 | 1.0000 | 0.0030 | 0.72 | 0.918 | 0.898 | 0.918 |
| 15 | LCT-017-012 | 0.99330 | 0.0002 | 1.0000 | 0.0030 | 0.67 | 0.923 | 0.903 | 0.922 |
| 16 | LCT-017-013 | 0.99205 | 0.0002 | 1.0000 | 0.0030 | 0.80 | 0.924 | 0.903 | 0.924 |
| 17 | LCT-017-014 | 0.99233 | 0.0002 | 1.0000 | 0.0030 | 0.77 | 0.928 | 0.907 | 0.929 |
| 18 | LCT-017-015 | 0.98925 | 0.0002 | 1.0000 | 0.0025 | 1.09 | 0.892 | 0.892 | 0.866 |
| 19 | LCT-017-016 | 0.99057 | 0.0002 | 1.0000 | 0.0025 | 0.95 | 0.900 | 0.898 | 0.874 |
| 20 | LCT-017-017 | 0.99164 | 0.0002 | 1.0000 | 0.0025 | 0.84 | 0.907 | 0.905 | 0.882 |
| 21 | LCT-017-019 | 0.99161 | 0.0002 | 1.0000 | 0.0025 | 0.85 | 0.912 | 0.911 | 0.887 |
| 22 | LCT-017-020 | 0.98969 | 0.0002 | 1.0000 | 0.0025 | 1.04 | 0.916 | 0.915 | 0.892 |
| 23 | LCT-017-021 | 0.98903 | 0.0002 | 1.0000 | 0.0025 | 1.11 | 0.919 | 0.917 | 0.895 |
| 24 | LCT-017-022 | 0.98801 | 0.0002 | 1.0000 | 0.0025 | 1.21 | 0.933 | 0.931 | 0.909 |
| 25 | LCT-017-023 | 0.99289 | 0.0002 | 1.0000 | 0.0025 | 0.72 | 0.904 | 0.902 | 0.880 |
| 26 | LCT-017-024 | 0.99361 | 0.0002 | 1.0000 | 0.0025 | 0.64 | 0.913 | 0.911 | 0.888 |
| 27 | LCT-017-025 | 0.99019 | 0.0002 | 1.0000 | 0.0025 | 0.99 | 0.911 | 0.908 | 0.890 |
| 28 | LCT-017-028 | 0.99069 | 0.0002 | 1.0000 | 0.0025 | 0.94 | 0.864 | 0.859 | 0.845 |
| 29 | LCT-017-029 | 0.99083 | 0.0002 | 1.0000 | 0.0025 | 0.93 | 0.874 | 0.868 | 0.857 |
| 30 | LCT-026-003 | 0.99995 | 0.0002 | 1.0000 | 0.0062 | 0.01 | 0.905 | 0.943 | 0.855 |
| 31 | LCT-040-010 | 0.98967 | 0.0002 | 1.0000 | 0.0046 | 1.04 | 0.977 | 0.952 | 0.979 |
| 32 | LCT-042-001 | 0.99057 | 0.0002 | 1.0000 | 0.0016 | 0.95 | 0.894 | 0.893 | 0.868 |
| 33 | LCT-042-002 | 0.99089 | 0.0002 | 1.0000 | 0.0016 | 0.92 | 0.894 | 0.893 | 0.869 |
| 34 | LCT-042-003 | 0.98973 | 0.0002 | 1.0000 | 0.0016 | 1.04 | 0.882 | 0.881 | 0.857 |
| 35 | LCT-042-004 | 0.99180 | 0.0002 | 1.0000 | 0.0017 | 0.83 | 0.873 | 0.872 | 0.848 |
| 36 | LCT-042-005 | 0.99212 | 0.0002 | 1.0000 | 0.0033 | 0.79 | 0.874 | 0.872 | 0.848 |
| 37 | LCT-042-006 | 0.99282 | 0.0002 | 1.0000 | 0.0016 | 0.72 | 0.880 | 0.878 | 0.854 |
| 38 | LCT-042-007 | 0.99010 | 0.0002 | 1.0000 | 0.0018 | 1.00 | 0.881 | 0.880 | 0.857 |
| 39 | LCT-049-001 | 0.99042 | 0.0002 | 1.0000 | 0.0011 | 0.97 | 0.761 | 0.793 | 0.690 |
| 40 | LCT-049-002 | 0.99136 | 0.0002 | 1.0000 | 0.0011 | 0.87 | 0.764 | 0.796 | 0.692 |
| 41 | LCT-049-003 | 0.99131 | 0.0002 | 1.0000 | 0.0011 | 0.88 | 0.744 | 0.775 | 0.674 |
| 42 | LCT-049-005 | 0.99056 | 0.0002 | 1.0000 | 0.0014 | 0.95 | 0.857 | 0.885 | 0.789 |
| 43 | LCT-049-006 | 0.99152 | 0.0002 | 1.0000 | 0.0014 | 0.86 | 0.859 | 0.888 | 0.790 |
| 44 | LCT-049-007 | 0.98999 | 0.0002 | 1.0000 | 0.0014 | 1.01 | 0.861 | 0.890 | 0.793 |
| 45 | LCT-049-008 | 0.99035 | 0.0002 | 1.0000 | 0.0012 | 0.97 | 0.847 | 0.875 | 0.780 |
| 46 | LCT-049-009 | 0.99061 | 0.0002 | 1.0000 | 0.0012 | 0.95 | 0.907 | 0.930 | 0.845 |
| 47 | LCT-049-010 | 0.99117 | 0.0002 | 1.0000 | 0.0012 | 0.89 | 0.908 | 0.932 | 0.846 |
| 48 | LCT-049-011 | 0.99038 | 0.0002 | 1.0000 | 0.0012 | 0.97 | 0.907 | 0.930 | 0.845 |
| 49 | LCT-049-012 | 0.99037 | 0.0002 | 1.0000 | 0.0012 | 0.97 | 0.898 | 0.921 | 0.837 |
| 50 | LCT-049-013 | 0.98920 | 0.0002 | 1.0000 | 0.0012 | 1.09 | 0.857 | 0.888 | 0.784 |
| 51 | LCT-049-015 | 0.99200 | 0.0002 | 1.0000 | 0.0012 | 0.81 | 0.853 | 0.885 | 0.782 |
| 52 | LCT-049-016 | 0.99071 | 0.0002 | 1.0000 | 0.0012 | 0.94 | 0.863 | 0.891 | 0.795 |
| 53 | LCT-049-017 | 0.99066 | 0.0002 | 1.0000 | 0.0012 | 0.94 | 0.846 | 0.873 | 0.779 |
| 54 | LCT-049-018 | 0.99455 | 0.0002 | 1.0000 | 0.0010 | 0.55 | 0.815 | 0.835 | 0.754 |

[a]With respect to LCT-050-001.
[b]With respect to LCT-079-002.
[c]With respect to LCT-079-007.

TABLE VI

FP Biases, Bias Uncertainties, Penalty, and 1-$\sigma$ Bounding Estimates for the TAD Canister*

| | $\beta$ | $\Delta\beta$ | $\lvert\beta\rvert + \Delta\beta$ | 1-$\sigma_{bound}$ |
|---|---|---|---|---|
| $^{149}$Sm (a) | −38.87 | 5.75 | 44.62 | 22.28 |
| $^{149}$Sm (b) | −33.49 | 5.95 | 39.43 | — |
| $^{103}$Rh (a) | 9.73 | 10.65 | 20.38 | 26.25 |
| $^{103}$Rh (b) | 16.75 | 9.22 | 25.97 | — |

*Note that (a) denotes weighting via $\hat{g}$ and (b) denotes the penalty-minimization scheme. All quantities are in units of pcm.

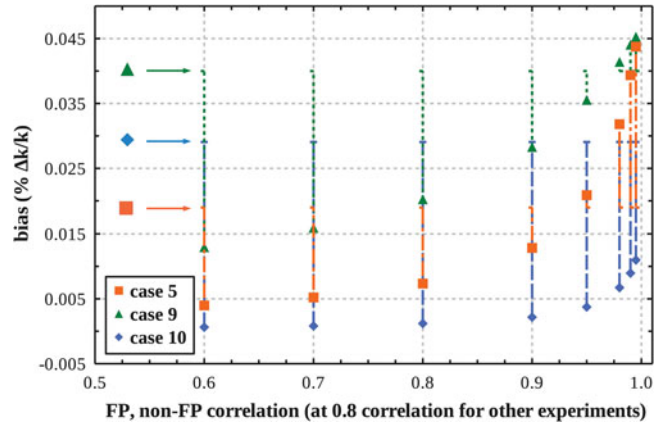


Fig. 2. The $^{103}$Rh bias as a function of $C_{FP/NFP}$.

The many assumptions notwithstanding, it is important to understand how the resulting partial biases behave to changes to the input values, namely, the assumed correlations between FP/NFP pairs and within the experiment series. To help determine such changes, we found the partial biases for varying FP/NFP or interseries correlations. Additionally, an approach for assessing statistical significance of the biases is discussed.

### *VI.A. FP/NFP Correlation*

To yield statistically significant partial biases, the uncertainty in the reactivity difference $\rho_{1\to2}$ between the FP and the NFP system must be small. Because the experimental uncertainties in the associated $k_{eff}$ values are typically significant, a high degree of correlation (i.e., shared uncertainty) is required to produce a small $\sigma_{\rho_{1\to2}}$. A good criteria for statistical significance may be that the magnitude of the partial bias must exceed the experimental uncertainty in the reactivity difference. Noting that the bias in the reactivity difference should be due mostly to the FP, then for the reactivity-difference bias and hence FP bias to be statistically significant, they should be larger than the uncertainty. This is the criterion used here for assessing statistical significance and could be a metric in future replacement experiments. Note that it may not be (and for the examples is not) the case that the only difference between the FP and the NFP systems is the FP (e.g., there exists a significant effect on $^{1}$H elastic scattering), and consequently, the bias in the reactivity difference may have other significant components. Similar effects in other experiments have been found when computing reactivity-difference sensitivities.[16] What this means is that a well-designed experiment pair should aim for both a small uncertainty and a configuration where any potential contribution to the bias due to the FP is large enough to be significant.

In the example above, the correlation between the FP and NFP experiments (henceforth, the FP/NFP correlation) was taken to be 0.98, which is substantial and likely too high. To see how the partial biases are affected by varying the assumed correlation, we computed the biases for several different correlation values ranging from 0.6 to 0.995. The results for three cases each for LCT-079 and LCT-050 are shown in Figs. 2 and 3, respectively. The error bars included extend from the calculated data point to the bounding 1-$\sigma$ value. The bounding estimate can be positive or negative; here, only the half closest to the maximum computed bias is included.

Of the three LCT-079 cases depicted in Fig. 2, both cases 9 and 10 have biases that significantly exceed the bounding estimates at a FP/NFP correlation of 0.98. At that value, the case 10 bias is just slightly above the bounding value whereas the case 9 bias is significantly beyond its bounding value. The case 5 bias is below its bounding value for all values of the the FP/NFP correlation. For all the cases, the biases grow most quickly for a correlation greater than 0.9. This demonstrates the impact a high correlation and hence low uncertainty in $\rho_{1\to2}$ has on the extracted bias.

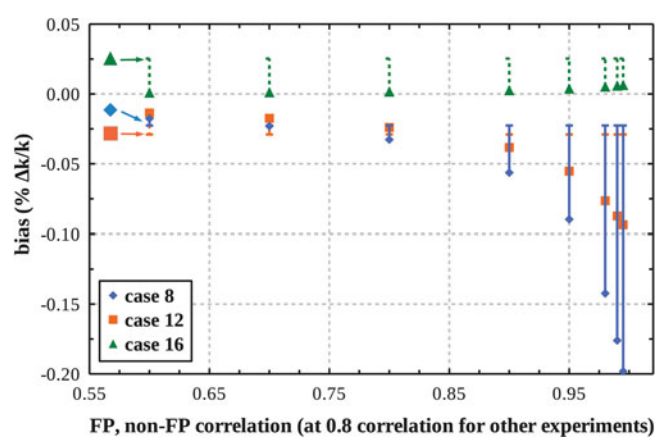


Fig. 3. The $^{149}$Sm bias as a function of $C_{FP/NFP}$.

For case 5, the reactivity-difference uncertainty is 32 pcm for a correlation of 0.98, and so, the computed bias at that point does not meet the given criterion for statistical significance. For cases 9 and 10, the experimental uncertainty for a correlation of 0.98 is 16 pcm, and both partial biases exceed this value significantly and so are statistically significant.

Of the LCT-050 cases depicted in Fig. 3, both cases 8 and 12 have biases that significantly exceed the bounding 1-$\sigma$ estimates, and this occurs for correlations as low as 0.8. The bias for case 16 never exceeds its bounding estimate. The biases at a correlation of 0.98 for all three cases shown exceed the reactivity-difference uncertainty of 16 pcm and thus are statistically significant.

Several of the LCT-050 cases and cases 8, 9, and 10 of the LCT-079 series exhibited biases that were beyond the 1-$\sigma$ estimates for a correlation of 0.98. This indicates that the correlation assumed is likely too high. A value of 0.9 or less is probably more realistic. A proper quantification of such correlations would be a valuable area of future work.

### *VI.B. Interseries Correlation*

It was further assumed in the examples that experiments within a given series had a correlation in their uncertainty of 0.8. This is probably a reasonable figure, but surely, each series has in reality a different correlation, and moreover, subsets within series will have correlations that vary along with the parameters of the experiment (e.g., water height or pitch).

To see the impact of this assumption on the partial biases, we ran several TSURFER cases with different interseries correlations as well as different FP/NFP correlations. The interseries correlation was varied by increments of 0.1 between 0.5 and 0.9. FP/NFP correlations of 0.8, 0.9, and 0.98 were investigated.

The LCT-079 cases are shown in Fig. 4. The partial biases for a FP/NFP correlation of 0.98 are most sensitive to the interseries experiment correlation. Case 9 is the least sensitive overall. A general negative trend in the bias with increasing interseries correlation is observed. For a FP/NFP of 0.98, the change from the maximum to the minimum bias was ~75% for case 5. For cases 9 and 10, the change from the maximum to the minimum was ~16% and 34%, respectively, both for a FP/NFP correlation of 0.98.

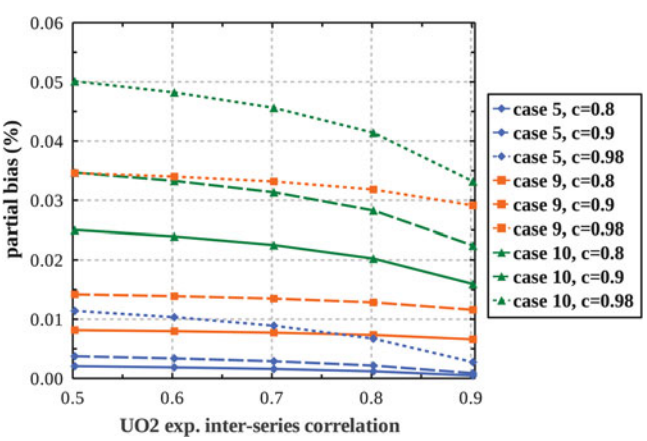


Fig. 4. The $^{103}$Rh bias as function of $C_{inter}$.

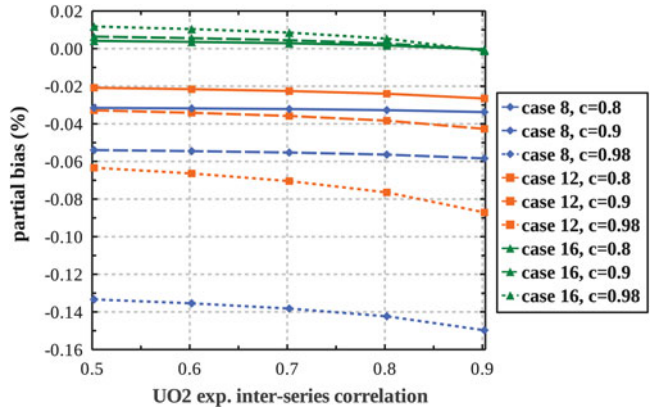


Fig. 5. The $^{149}$Sm bias as function of $C_{inter}$.

The LCT-050 cases are shown in Fig. 5. The samarium partial biases show about the same dependence on the interseries correlation as the rhodium cases, i.e., a general negative trend with increasing interseries correlation. However, because the biases are largely negative to begin with, the dependence serves to increase the magnitude of the biases. The maximum change in the biases is observed for a FP/NFP correlation of 0.98, with the case 12 bias increasing in magnitude by 37%.

## VII. CONCLUSION

This paper has presented new methods to facilitate determination and application of partial biases to application systems in criticality safety analyses.

An approach using GLLSM and reactivity-difference sensitivities to isolate partial biases was outlined and applied to the LCT-050 and LCT-079 experiment series.

Additionally, sensitivity and uncertainty analysis was then used to adjust partial biases to yield biases appropriate for the application system. A penalty was developed to account for dissimilarity between the application and experiment system $k_{eff}$ sensitivities to the FP cross section. Two weighting schemes were presented for producing a single application from several single partial biases.

Finally, a brief analysis was performed to assess the dependence of the partial bias on two key assumptions, namely, the correlation between a FP and a NFP experiment pair and the correlation of experiments within a

given series. Partial bias statistical significance was also discussed.

Future work should focus on generating a greater volume and depth of correlation data for extant critical experiments. Without such data, the value of data adjustment as a tool for extracting partial biases (and consequently the value of those biases) is severely limited.

Additionally, work should be done to use S/U data and parameters in robust optimization of future critical experiments. Initial (small-scale) scoping studies have been performed that use $p_{ds}$ as an objective function for one FP of interest, but such problems should be implemented with full constraints and solved on large-scale systems for the value of the method to be assessed fully.

## ACKNOWLEDGMENTS

The first author was supported by the U.S. Department of Energy's (DOE's) Advanced Fuel Cycle Initiative University Fellowship Program. The second author was supported by DOE's Nuclear Criticality Safety Program.

## REFERENCES

1. ANSI/ANS-8.1-1998, "Nuclear Criticality Safety in Operations with Fissionable Material Outside Reactors," American Nuclear Society, La Grange Park, Illinois (1998).

2. ANSI/ANS-8.24-2007, "Validation of Neutron Transport Methods for Nuclear Criticality Safety Calculations," American Nuclear Society, La Grange Park, Illinois (2007).

3. B. L. BROADHEAD, C. M. HOPPER, and C. V. PARKS, "Sensitivity and Uncertainty Analyses Applied to Criticality Validation," NUREG/CR-6655, Vols. 1 and 2 (ORNL/TM-13692/V1 and V2), U.S. Nuclear Regulatory Commission, Oak Ridge National Laboratory (Nov. 1999).

4. C. V. PARKS, J. C. WAGNER, and D. E. MUELLER, "Full Burnup Credit in Transport and Storage Casks: Benefits and Implementation," *Radwaste Solutions*, **14**, *2*, 32 (2007).

5. B. T. REARDEN and D. E. MUELLER, "Recent Use of Covariance Data for Criticality Safety Assessment," *Nucl. Data Sheets*, **109**, *12*, 2739 (2008).

6. SCALE: A Modular Code System for Performing Standardized Computer Analyses for Licensing Evaluation," ORNL/TM-2009/39, Version 6.0, Vols. I, II, and III (2009); Available as CCC-750, Radiation Safety Information Computational Center at Oak Ridge National Laboratory.

7. M. L. WILLIAMS, "Sensitivity and Uncertainty Analysis for Eigenvalue-Difference Responses," *Nucl. Sci. Eng.*, **155**, 18 (2007).

8. S. GOLUOGLU, C. M. HOPPER, and B. T. REARDEN, "Extended Interpretation of Sensitivity Data for Benchmark Areas of Applicability," *Trans. Am. Nucl. Soc.*, **88**, 77 (2003).

9. B. L. BROADHEAD, B. T. REARDEN, C. M. HOPPER, J. J. WAGSCHAL, and C. V. PARKS, "Sensitivity- and Uncertainty-Based Criticality Safety Validation Techniques," *Nucl. Sci. Eng.*, **146**, 340 (2004).

10. B. T. REARDEN, M. L. WILLIAMS, M. A. JESSE, D. E. MUELLER, and D. A. WIARDA, "Sensitivity and Uncertainty Analysis Capabilities and Data in Scale," *Nucl. Technol.*, **174**, 236 (2011).

11. J. A. ROBERTS, P. P. W. WILSON, and D. E. MUELLER, "Further Intrepretation of Sensitivity Data in Support of Burnup Credit," In *Proc. Nuclear Criticality Safety Division Topl. Mtg. Realism, Robustness, and the Nuclear Renaissance*, Richland, Washington, September 13–17, 2009. American Nuclear Society (2009) (CD-ROM).

12. M. C. FERRIS, O. L. MANGASARIAN, and S. J. WRIGHT, *Linear Programming with MATLAB*, Society for Industrial and Applied Mathematics, Philadelphia, Pennsylvania (2007).

13. *International Handbook of Evaluated Criticality Safety Benchmark Experiments*, NEA/NSC/DOC(95)03/I-VIII, Organisation for Economic Co-operation and Development/Nuclear Energy Agency (Sept. 2007).

14. "Transportation, Aging, and Disposal Canister System Performance Specification," U.S. Department of Energy, Office of Civilian Radioactive Waste Management.

15. T. T. IVANOVA, M. N. NIKOLAEV, K. F. RASKACH, E. V. ROZHIKHIN, and A. M. TSIBOULIA, "Influence of the Correlations of Experimental Uncertainties on Criticality Prediction," *Nucl. Sci. Technol.*, **145**, *1*, 97 (2003).

16. N. LECLAIRE, T. IVANOVA, E. LÉTANG, E. GIRAULT, and J. F. THRO, "Fission Product Experimental Program: Validation and Computational Analysis," *Nucl. Sci. Eng.*, **161**, 188 (2009).